The impacts of secondary ice production on the microphysics and dynamics of mid-latitude cold season convection

Reviewer #2

General Comments:

This is a well-written manuscript with clear objectives, descriptions of the observations and comparison of observations with model results. I also appreciate the effort to explain and address common pitfalls of FFD parameterizations on lines 170-182. The conclusions are generally supported by the observations and analysis presented. I have some minor revisions and comments, which I hope will clarify some missing details and add some much-needed discussion to the paper.

We deeply appreciate your comments for helping to improve this manuscript! Please see our responses to your questions below (in blue).

Minor comments:

1. While the authors focus on the effects of the HM and FFD processes on ice number the IWC in clouds, can other SIP mechanisms such as ice-ice collisions and fragmentation also contribute/complement the HM and FFD processes? For example, Zhao and Liu (2021) showed that the addition of SIP process parameterization such as ice-ice collision fragmentation and droplet shattering during freezing can increase global ice water path by 20% in the CAM6 model. Is it possible that including other SIP process parameterizations may change the result that the F9-HMgc-FFD performs best compared to the BASE, and HMgr-FFD for Flight 9?

Thank you very much for this suggestion. We recently implemented the ice-ice collision break-up (CB) process and tested its impact on the simulation results, following Phillips et al. 2017. We make additional adjustment to the method by limiting the collision breakup only to the situation when the relative velocity between two ice particles is larger than 1 m s^{-1} (Hoarau et al. 2018, Korolev and Leisner, 2020).

For Flight 9, including CB further increases N_i at various altitudes and can potentially lead to an unrealistic surge in ice splinter production near the surface due to the rapid FFD rate. To address this issue, we implemented a correction to the FFD process based on the recommendations of Lachapelle et al. (2025). The SIP rate for FFD follows the original exponent-4 approach (Eq. 3), but is capped when D exceeds 1878.2 μm. Additionally, a linear temperature dependence is applied, with an actual rate (N_f) rate at –12.5°C which will be scaled down ($c*N_f$) to zero at –25°C and –2°C (c is a T dependent linear scaling factor between 0 and 1).

The additional simulation with three SIP processes included in this manuscript under the experiment "HMgc-FFDl-CB," where FFDl refers to FFD at lower rates (as opposed to the original higher rate, FFDh). CB denotes ice–ice collisional breakup.

The new experiment incorporating all three SIP processes (green dashed lines) yields results similar to the HMgc-FFDh simulation (red lines), which uses the same HM process and a

higher FFD rate. We observed that applying the higher FFD rate (original approach, not shown) in combination with both HM and CB processes leads to a significant increase in N_i near the surface, as both HM and CB processes produce large numbers of ice splinters that further enhance FFD. However, such extremely high values of N_i were not observed in the actual data. In the new experiment, the use of the reduced FFD rate prevented this explosive increase in N_i near the surface. This suggests that the FFD rate based on Lawson et al. may be overestimated, while the reduction proposed by Lachapelle et al. (2025) improves the agreement between simulations and observations.

Here is a revised Fig. 5 (new experiment results in green dashed line) for F9:

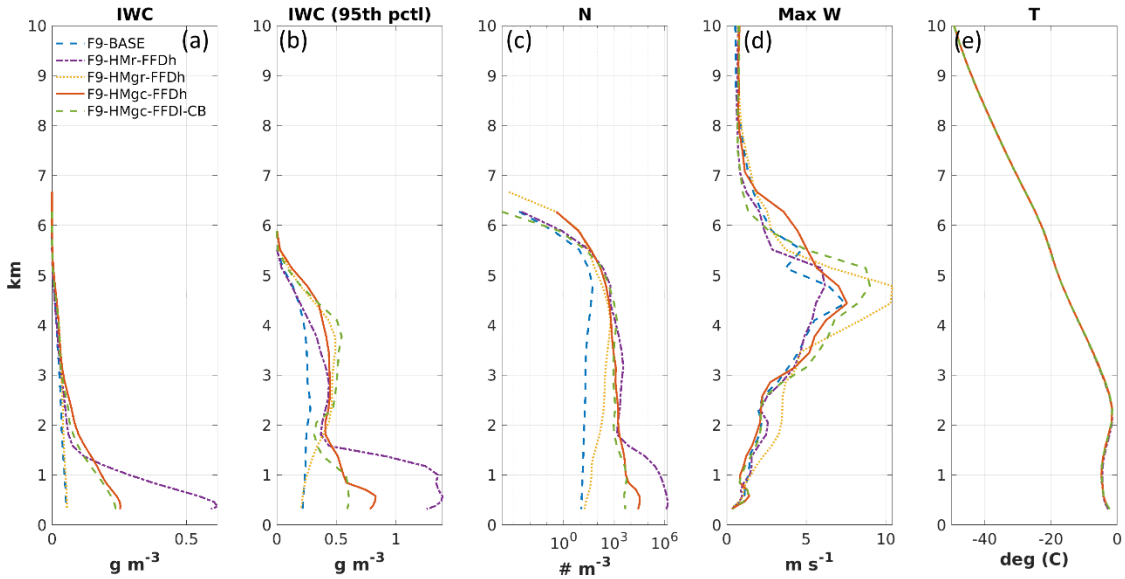

Figure 5. Profiles from the baseline and SIP simulations on 2019-02-07 for the case of ICICLE Flight 9. (a): mean IWC, (b): 95 percentile of IWC (99th pctl of IWC), (c): mean Ni with the number of ice particle smaller than 40 μm excluded, (d): maximum vertical wind speed (wmax), (d) T (the three simulations have only slightly different temperature that is not distinguishable in the figure). All profiles are calculated from simulation results at 510 min (20:30 UTC) after the initiation time of 12:00 UTC. All profiles are calculated for the region within 10 km of distance to the aircraft track.

An additional paragraph was added into the manuscript:

"Including the CB process in the experiment led to an explosive increase in FFD rates near the surface (not shown). To mitigate this, we applied the FFDl (lower rate) parameterization, as proposed by Lachapelle et al. (2025). Results from the three-process experiment (F9-HMgc-FFDl-CB) were similar to those of F9-HMgc-FFDh in terms of N_i, IWC, LWC, and Z_{median}. The CB process (types I, II, and III) produced positive SIP rates at multiple altitudes, including levels below 2 km (Figure 6f, 6g), potentially further activating the FFD process. The use of the FFDl parameterization effectively suppressed near-surface FFD rates, resulting in values that were substantially lower than the explosive rates simulated in F9-HMr-FFDh (purple dashed lines)."

Similar conclusion for Fig. 6. The panels f and g show the SIP rate from ice-ice collisional breakup for type I (involve graupel and hail only), and for type II & III (involve snow/ice crystal with/without graupel and hail).

Here is a revised Fig. 6 (new experiment results in green dashed line) for F9:

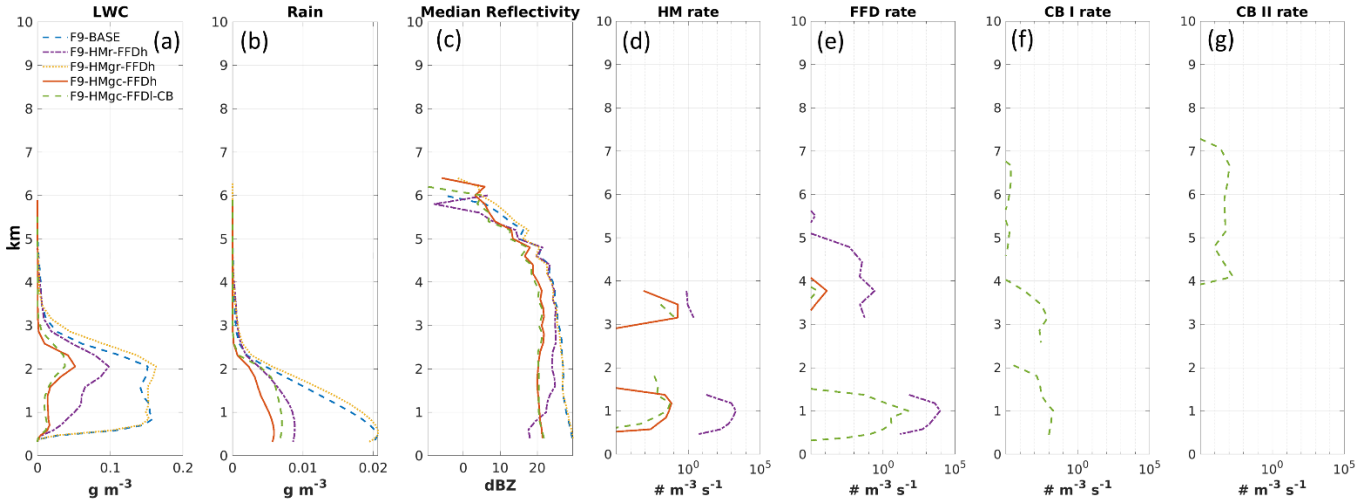

Figure 6. Profiles from the baseline and SIP simulations on 2019-02-07. (a): mean LWC, (b): mean RWC, (c): median radar reflectivity (Zmedian), (d): mean Hallett-Mossop rate, (e): mean Fragmentation of Freezing Drop rate, (f): ice-ice collisional breakup rate (type I), (g): ice-ice collisional breakup rate (type II & III) All profiles are calculated for the region within 10 km of distance to the aircraft track and at 20:30 UTC.

Here is a revised Fig. 7 (new experiment results in green dashed line) for F9:

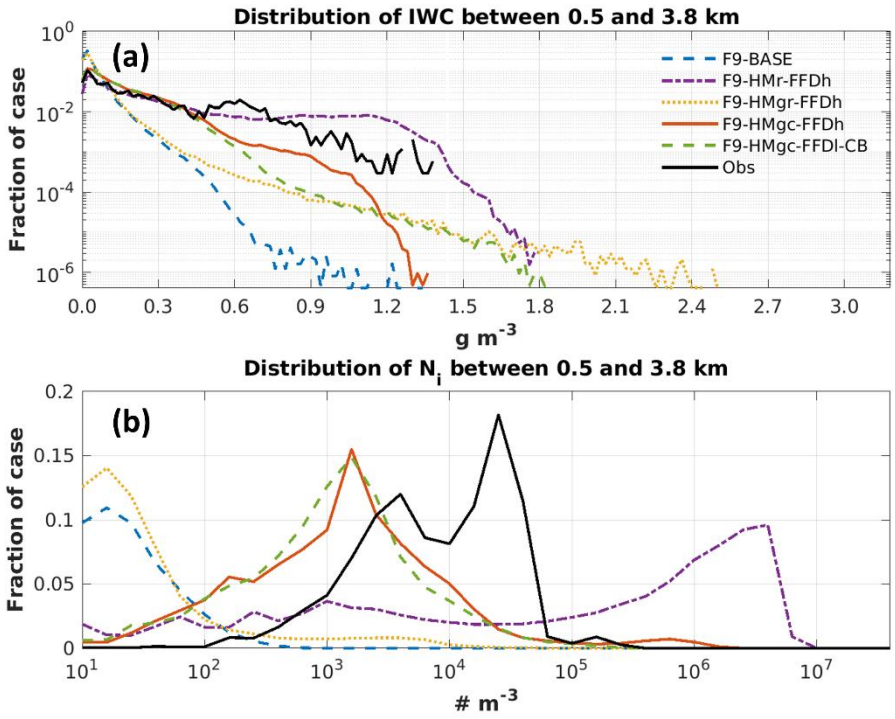

Figure 7. Distribution of IWC (a) and Ni with the number of ice particle smaller than 40 μm excluded (b) for model simulations at 20:30 UTC on 2019-02-07 and for the observation data for ICICLE Flight 9 between 20:00 and 21:00 UTC. The results from model simulations are calculated for altitudes between 0.5 and 5.5 km and with ice water content higher than 0.001 g m-3 in the region within 20 km of distance to the aircraft track. The results from in situ observation are calculated for the condition with IWC higher than 0.001 g m-3. (b): logarithmic bin width of 1/5 of an order of magnitude is used. Blue dashed lines: Baseline simulation, purple dash-dot line: SIP (F9-HMr-FFDh), yellow dotted lines: SIP (F9-HMgr-FFDh) simulation, red lines: SIP (F9-HMgc-FFDh) simulation, green dashed lines: SIP (F9-HMgc-FFDl-CB), black lines: observation.

The new experiment (green dashed lines) produces similar N_i distribution with the cases of extreme high N_i (>2x10^5 m^{-3}) reduced even compared to HMgc-FFDh (red line).

Reference:

Hoarau, T., Pinty, J.-P., and Barthe, 455 C.: A representation of the collisional ice break-up process in the two-moment microphysics LIMA v1.0 scheme of Meso-NH, Geoscientific Model Development, 11, 4269–4289, https://doi.org/10.5194/gmd-11-4269-2018, 2018.

Korolev, A. and Leisner, T.: Review of experimental studies of secondary ice production, Atmospheric Chemistry and Physics, 20, 11 767–11 797, https://doi.org/10.5194/acp-20-11767-2020, 2020.

Lachapelle, M., Nichman, L., Girouard, M., Nguyen, C., Ranjbar, K., Bliankinshtein, N., Bala, K., Thériault, J.M., French, J. R., Minder, J. R., Wolde, M.: Airborne and ground measurements for vertical profiling of secondary ice production during ice pellet precipitation J Atmos Sci, 10.1175/jas-d-24-0117.1, 2025.

Phillips, V. T. J., Yano, J.-I., and Khain, A.: 1. Ice Multiplication by Breakup in Ice–Ice Collisions. Part I: Theoretical Formulation, J. Atmos. Sci., 74, 1705–1719, https://doi.org/10.1175/JAS-D-16-0224.1, 2017b.

2. Line 390: The Flight 20 case is a little confusing. The authors mention that the system primarily consisted of stratiform clouds, but Fig. 12 suggests a deeper system with cloud top heights near 8-9 km above ground. Also, the method of ice formation is claimed to be primarily homogenous freezing and precipitation of ice particles from above. It isn't clear from Fig 12 radar data if such ice precipitation is observed. Could the authors provide more details regarding the claim of Ni primarily from precipitating ice vs heterogeneous freezing within the storm system?

Thank you for this comment! After further analyzing the data, we changed our claim here.

Thank you for this comment! After further analyzing the data, we changed our claim here, and added discussions below in the manuscript:

"One possible reason for the fairly accurate N_i values in the F20-BASE simulation is that in this stratiform case N_i is likely governed by the heterogeneous nucleation process, with SIP playing a relatively less important role. In the F20-BASE simulation, most N_i values between –15°C and –25°C (T of the maximal flight altitude for Flight 20 at ~6.4 km) are higher than the parameterized N_i due to condensation freezing/deposition ice nucleation (lower half of the small red cycles in Figure 18a) within the same temperature range, but lower than the parameterized N_i for colder temperatures (upper half of the small red cycles in Figure 18a). Ice particles formed at temperatures below –25°C through heterogenous nucleation may gradually fall to warmer, lower-altitude regions, thereby contributing to higher N_i compared to the parameterized N_i. Additionally, simulated results from F20-BASE (Figure 18a) show a gradual decrease in N_i with increasing temperature, underscoring the effect of ice particle aggregation.

In the case of Flight 20, the cloud top extends above the homogeneous freezing threshold at -40°C, allowing for the possibility that homogeneous ice nucleation could also influence N_i at lower altitudes as these ice particles descend. However, as shown in Figures 18a, the N_i values above the -40°C level are not substantially higher than most N_i values seen between -20°C and -30°C (ranging from 10^3 to 10^5 m^{-3}). As ice particles formed through homogeneous freezing descend into warmer temperatures, aggregation processes are expected to further decrease Ni, resulting in concentrations lower than those shown between –20 °C and –30 °C in Figure 18a, where most values range from 10^3 to 10^5 m^{-3}. This pattern indicates that, at temperatures warmer than -25°C, the ice particle concentrations are more likely dominated by heterogeneous nucleation rather than by the effects of homogeneous nucleation.

Compared to F20-BASE (Figure 18a), F20-HMgc-FFDh (Figure 18b) and F20-HMgc-FFDl-CB (Figure 18c) have more frequent occurrences of higher N_i values for temperatures above –10°C, indicating the influence of SIP. However, these impacts remain moderate.

In the observed N_i frequency distribution (Figure 18d), two distinct clusters are apparent. One cluster (indicated by the large red circle) aligns closely with the parameterized N_i line, suggesting the influence of heterogeneous ice nucleation. The second cluster, which exhibits higher N_i values below –20°C, may indicate the presence of falling ice particles originating

from higher altitudes, regions that were not directly observed due to the flight's altitude limitations. The higher N_i values may also result from the effects of SIP. However, N_i gradually decreases with increasing temperature. Unlike the F20-HMgc-FFDh (Figure 18b) and F20-HMgc-FFDl-CB (Figure 18c) cases, there is no distinct 'protruding' cluster (green circles in Figure 18b, 18c) that would indicate a sudden N_i increase at lower altitudes due to SIP. Thus, ice formation in warmer regions (lower altitudes) in Figure 18c is likely dominated by heterogeneous nucleation, although the influence of SIP cannot be ruled out.

Observed N_i values at T > –20°C (Figure 18c, $N_i > 1 \times 10^4$ m $^{-3}$) are frequently higher than those in the simulations (Figures 18a, 18b and 18c, where N_i mostly ranges between 1×10^3 and 1×10^4 m^{-3}). This discrepancy warrants further investigation into the uncertainties associated with the parameterized heterogeneous nucleation at colder temperatures (T < –20°C), the ice–ice collection efficiency and SIP."

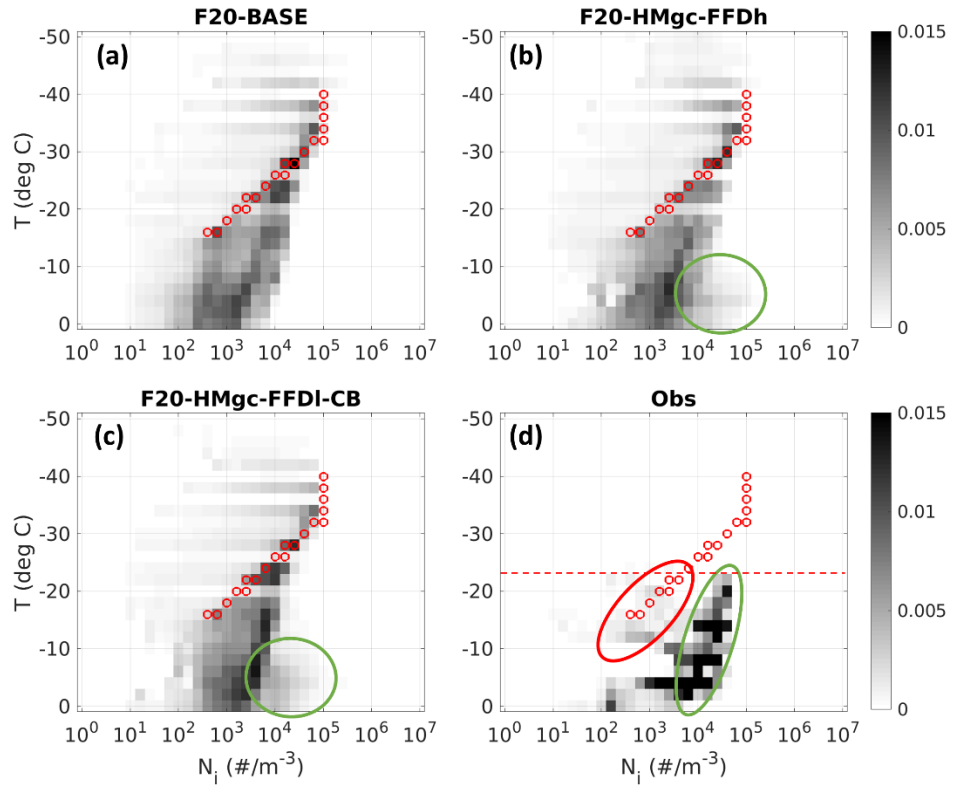

Figure 18: 2D histograms for the frequency of Ni regarding the T for F20-BASE (panel a), F20-HMgc-FFDh (panel b), F20-HMgc-FFDl-CB (panel c), and the observation for Flight 20 (panel d). Small red cycles: parameterized N_i due to condensation freezing/deposition ice nucleation (adapted from Cooper, 1986). Red dashed line: minimal flight T between 12:30 and 16:00 UTC.

3. Line 425: Can the authors expand on the reasoning why storm system longevity might contribute to HIWC? Does a growing ice particle feel the storm system lifetime? At first thought, it should fall out of the cloud whenever it gets too heavy, and stronger updrafts should help it stay afloat longer and get bigger. This suggests that stronger updrafts may result in larger ice particles, yet Fig 19 suggests that larger ice particles were observed during weaker updraft conditions. Some explanation/clarification will better help the readers since these are very interesting results.

This is a great question! We have several hypotheses to explain the differences. These discussions are added into the manuscript:

"In the Cayenne case (tropical setting), the storm system exhibits much stronger convection, with more intense turbulence and updrafts, which in turn enhances SIP processes. For instance, vigorous updrafts and abundant supercooled liquid water near the melting layer increase the mixing of liquid droplets and ice particles, thereby boosting both HM and FFD rates. Turbulence further amplifies the efficiency of CB. Overall, the N_i in the tropical case (Cayenne) is higher than in the mid-latitude winter cases (ICICLE F9 and F20), resulting in a size distribution that is more heavily weighted toward smaller particles for Cayenne.

Strong updrafts in tropical mesoscale systems limit the growth time of ice particles, as many are rapidly transported to higher altitudes. While these vigorous updrafts can promote the formation of rimed particles such as graupel and hail, such particles are generally confined to localized regions within the storm, and the majority of ice in tropical systems consists of smaller ice particles. In contrast, ice particles in mid-latitude winter nimbostratus clouds tend to have longer residence times, allowing for more favorable conditions for depositional growth and aggregation. As a result, aggregation processes are more dominant in mid-latitude winter storms, leading to a greater abundance of larger snow aggregates.

Note that although the fraction of smaller ice particles in the Cayenne case is higher than in ICICLE F20, the total IWC in the Cayenne case is actually greater, with some extreme values exceeding 3 g m^{-3}, levels not observed in ICICLE F20."

4. Line 435: Could HIWC be influenced by higher and lower aerosol number concentrations during the French Guiana, ICICLE F09 and F20 flights? Could aerosol cleansing during a longer storm increase supersaturation fluctuations to form bigger ice particles during F20?

In a recent experiment using GEM for the French Guiana case, we reduced the background aerosol number concentration from the default value in the P3 scheme (300 cm^{-3}) to 80 cm^{-3}. This adjustment led to a decrease in liquid drop number concentration, and although the LWC also decreased, it did so less significantly, resulting in generally larger liquid drops. Because the FFD process accelerates with increasing drop size (being proportional to D^4), this produced higher N_i values. However, the impact on IWC was mixed: a decrease was observed below 8 km, while an increase occurred above 8 km. These results suggest that aerosols do influence cloud microphysical processes, but further studies are needed to fully understand their potential impacts.

Minor corrections:

Line 113: How thick is the observed melting layer for F09 and F20? What is the model vertical resolution and is it able to resolve the melting layer for each grid size?

Radar observations indicate that the melting layers for both flights occur at roughly the same altitude, around 2 km, with a thickness between approximately 200 and 500 m. The model's vertical resolution at this altitude is about 250 m, which should be sufficient to resolve the melting layer. In Fig. 17 (or Fig. 18 in the revised version), the enhanced reflectivity associated with the melting layer is clearly identifiable near 2 km altitude.

Line 149: Is this a typo? The HM peak is at -5 C, and also goes to 0 at -5 C, Should it be -8 C?

Sorry about the confusion. This is a typo indeed. We changed the text into:

*"The parameterized HM process follows Hallet and Mossop (1974) stating the production of a peak value of 350 ice splinter per mg of collected liquid water during riming of liquid cloud drops or rains droplets within a temperature range of -3°C > T > -8°C, with the peak value at -5°C and varying linearly to 0 at -3°C and ~~-5~~ **-8** °C."*

Line 164: What is numerical value with units of the max Nf rate at T = -12.5 C?

The maximum rate of N_f at T=-12.5°C is the value directly calculated by Eq. 3 which depends on the size of the liquid drop (D). This N_f will then be linearly scaled down to zero at T=-25°C and T=-2°C. We updated the description:

"Following Keinert et al. (2020) the activity of the FFD process was limited to the temperature range -25°C < T < -2°C with a maximal rate of N_f (as calculated by Eq. 3, with or without capping) at T = -12.5°C. N_f is then linearly scaled down to zero as the temperature decreases from −12.5°C to −25°C or increases from −12.5°C to −2°C, according to a T dependent scaling factor c (where $c \in [0,1]$), such that the rate is $c \times N_f$. All newly produced ice splinters have a diameter of 10 µm."

Line 173: The "which collect rain droplets" makes the sentence a little difficult to read.

Thanks for this suggestion. We would like to retain this specification, as omitting "that collected the rain" could be misleading. There are multiple ice categories, and not all are involved in rain collection as referenced here.

"Excluding the mass of ice splinters, which typically represents a small fraction of the rain mass, the remaining rain mass is added to the ice category that collected the rain."

Fig 2: Can the F09 track also be overlayed on this figure? It will help the reader locate flight observations, the storm system and model grid centers better.

Thanks for this suggestion! Please find below the updated Fig. 2 and Fig. 11, with the flight tracks shown as green lines.

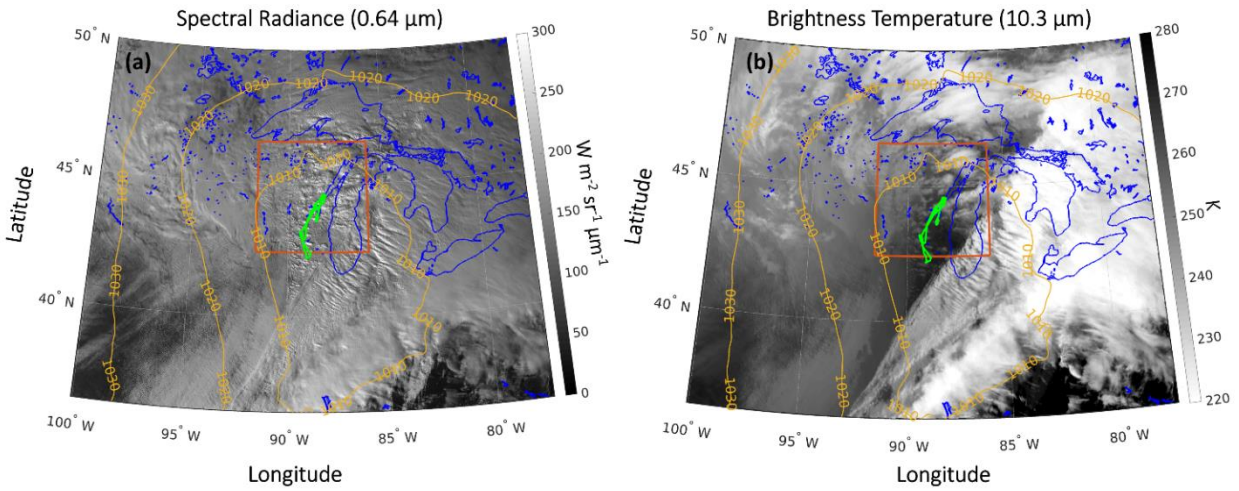

Figure 2. (a) GOES-16 spectral radiance at 0.64 µm (Channel 2). (b) GOES-16 brightness temperature at 10.3 µm (Channel 13). Both images are from 20:30 UTC on 9 February 2019. Blue lines denote coastlines and lakes; the red rectangle indicates the inner-most simulation domain (with a 0.25 km grid spacing) for Flight 9; yellow lines show the sea level pressure isobar at 18:00 UTC from the operational regional analysis used at ECCC; green lines: aircraft flight track. (Only data from the flight segments in the northern portion of the track were used in this study).

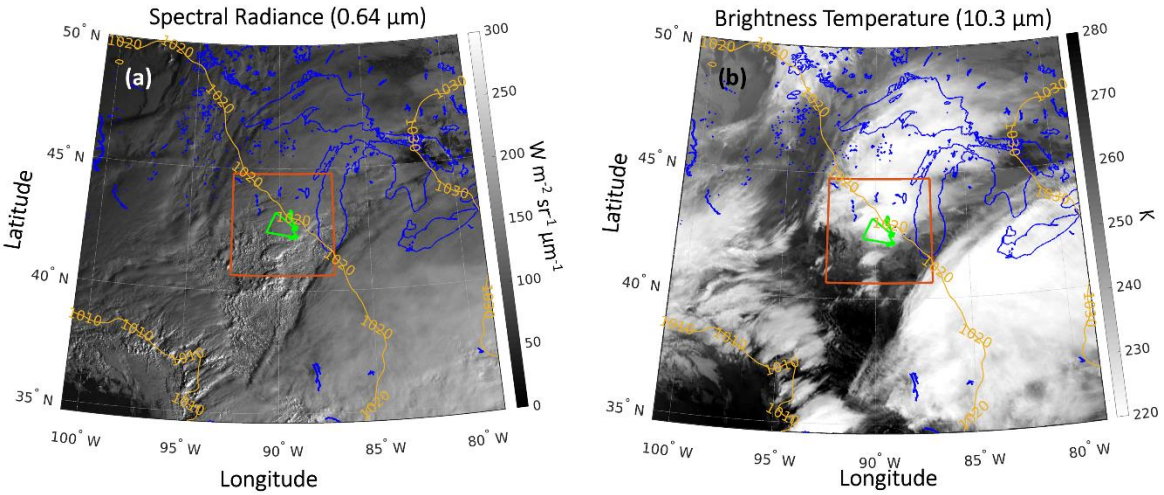

Figure 12. (a) GOES-16 spectral radiance at 0.64 µm (channel 2). (b) GOES-16 brightness temperature at 10.3 µm (channel 13). Both images are from 14:30 UTC on 23 February 2019. Blue lines represent coastlines, green lines represent aircraft flight track, and the red rectangle represents the inner-most simulation domain at 0.25 km resolution for Flight 20.

Flight 224: "The simulated brightness temperature closely matches the GOES-16 observations." With the naked eye, the GOES-16 temperature looks lower for the cloud system. Could you provide mean temp values for both for the cloud system?

> *Figure 4 is intended to illustrate how GEM simulates sea-level pressure and cloud cover at the synoptic scale. The model outputs shown here are from a simulation at lower horizontal resolution (2.5 km), as the 0.25 km resolution domain is too limited for this scale of comparison. As you also observed, there is a brightness temperature bias in the simulated results when compared to GOES-16 values. Investigations into the cause of this bias are*

ongoing. However, presenting the brightness temperature bias at 2.5 km resolution may be beyond the scope of this paper. We have added a clarification in the manuscript:

"The simulated brightness temperature at 10.3 μm closely matches the GOES-16 observations. However, a positive bias (indicating warmer values) is evident compared to the satellite data. Investigations into the cause of this bias are currently underway. Additionally, the simulation slightly underestimates cloud coverage over the southern part of Lake Michigan and in the southeastern corner of the simulation domain."

Line 304: It isn't clear exactly where the enhancement is occurring in the figure. Could you add a box/arrow to point at the regions?

The enhancement region is indicated by the white circles in the updated Fig. 10 (previously Fig. 9) (now the results of HMgc-FFDl-CB are also included):

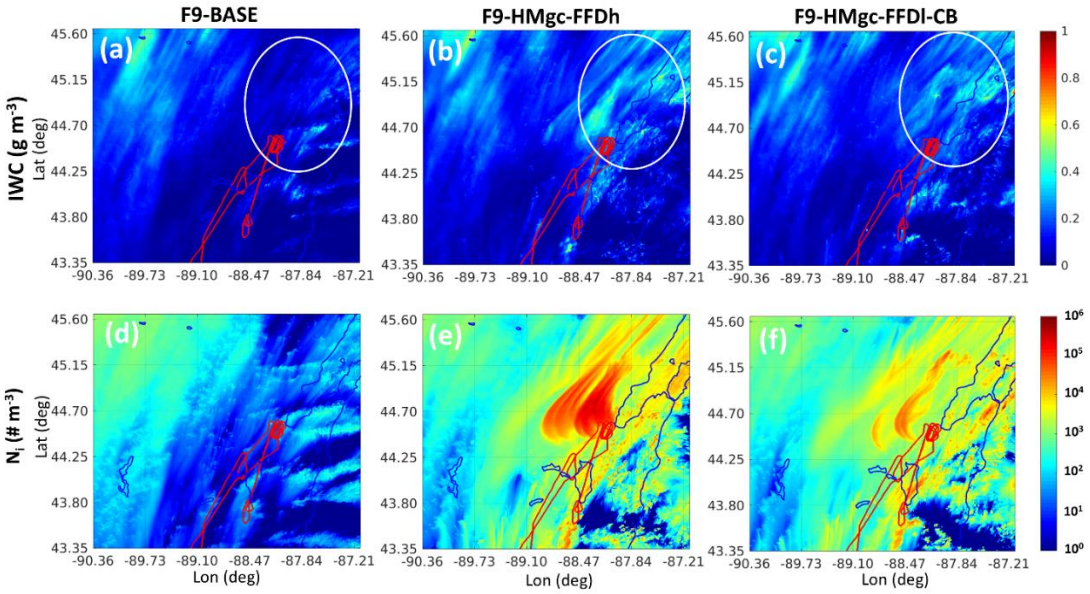

Figure 10. Averaged values between altitude of 0.5 and 3.8 km for Flight 9. (a), (b), (c): IWC; (d), (e), (f): Ni. First column for F9-BASE, middle column for F9-HMgc-FFD, third column for F9-HMgc-FFDl-CB. Red line: flight track.

Line 315: Also unclear where the increase in IWC is to be seen. The scale is massive and the difference in shades of grey is tough to spot.

The enhancement region is highlighted by the white circles in the updated Fig. 11 (previously Fig. 10) (now the results of HMgc-FFDl-CB are also included):

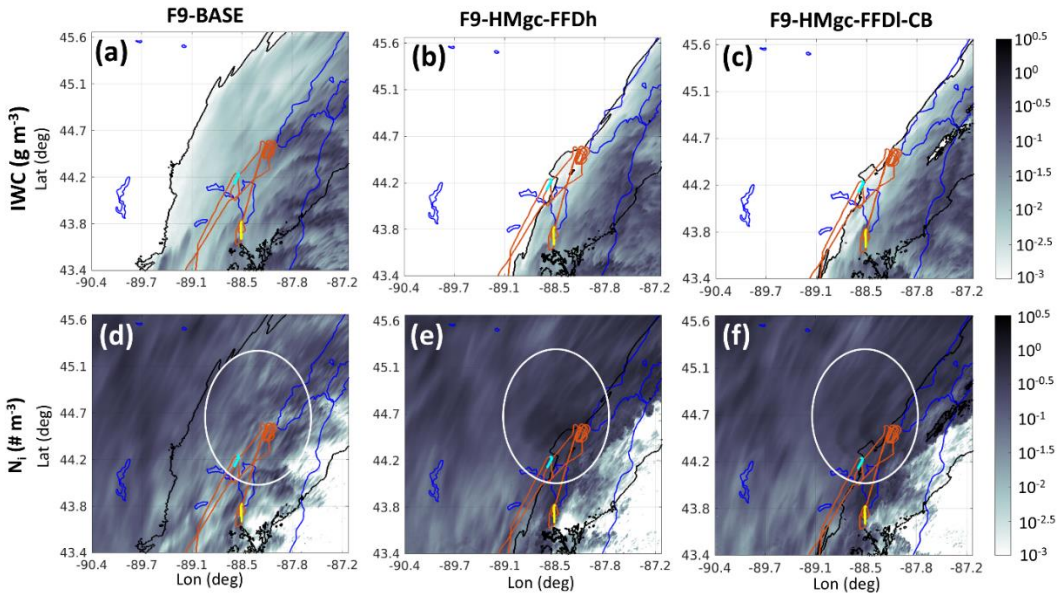

Figure 11. RWC (a, b, c) and IWC (d, e, f) near the surface for F9-BASE (a, d), F9-HMgc-FFDh (b, e) and F9-HMgc-FFDl-CB (c, f) simulations at 20:30 UTC on 2019-02-07. Black contour: region of freezing rain (RWC > 0.01 g m-3 and T < 0°C in the lowest model layer at ~20 m above surface). Red lines: Flight 9 aircraft track. Yellow lines: part of flight track below 800 m of altitude observing both supercooled liquid and ice near 20:12 UTC. Turquoise lines: part of flight track below 800 m of altitude observing only ice near 20:47 UTC.